Dynamics and threshold behaviour in polymer fibre bragg grating creation

Author:
Peng, Gang-Ding; Liu, Huiyong; Chu, Pak

Publication details:
Photorefractive fiber and crystal devices: materials, optical properties, and applications VIII
pp. 164-178
0819445711 (ISBN)

Event details:
SPIE'2002
USA

Publication Date:
2002

Publisher DOI:
http://dx.doi.org/10.1117/12.453586

Dynamics and Threshold Behaviour in Polymer Fibre Bragg Grating Creation

Gang-Ding Peng, Hui Yong Liu, and Pak Lim Chu*

Photonics and Optical Communications Group
School of Electrical Engineering & Telecommunications
The University of New South Wales, Sydney 2052, Australia

Phone: 612 9385 4014, Fax: 612 9385 5993, Email: g.peng@unsw.edu.au

*The Optoelectronic Research Centre
City University of Hong Kong,
Tat Chee Avenue, Kowloon, Hong Kong

Abstract

Photosensitivity has been observed and Bragg gratings have been created in various polymer optical fibres in recent years. Nevertheless the mechanisms of Bragg grating formation in polymer optical fibres are yet to be fully investigated and understood. We carried out experimental investigations on the dynamic growth of Bragg grating under various exposure conditions. For the first time, we observed clearly a threshold behaviour in the grating creation process. The threshold distinguishes two types of fibre gratings that have quite differently properties and performance.

Key words: Polymer optical fibre, fibre Bragg grating, photosensitivity.

1. Introduction

Fibre Bragg grating technology has fully developed and has found many important applications in optical communication systems and optical fibre sensor systems, since the early days that the photosensitivity in silica fibre was observed by Hill et al in 1978 [1]. Fibre Bragg gratings have many attractive attributes over their conventional bulk counterparts such as their compactness, stability, portability, high power efficiency (low insertion loss and low connection loss) and hence overall better system performance. In optical fibre communication systems, fibre Bragg gratings could be used as key components such as dispersion compensator, optical add-drop multiplexer, wavelength filter, pulse reshaping filter, etc. [2-4]. In optical fibre sensor systems, fibre Bragg gratings could be used as sensing elements for measurement, monitoring or characterisation of strain, temperature, sound, pressure, etc [5].

Photorefractive Fiber and Crystal Devices: Materials, Optical Properties, and Applications VIII,
Francis T. S. Yu, Ruyan Guo, Editors, Proceedings of SPIE Vol. 4803 (2002)

Irradiation of the core of an optical fibre with ultraviolet light introduces a permanent change in the refractive index. This photorefractive effect, referred to as photosensitivity, has great practical significance because it makes possible the creation of fibre Bragg grating. Photosensitivity of PMMA has been studied for about 30 year if not longer. The earliest report we found on photosensitivity of PMMA is the work of Tomlinson et al [6]. In their work, they found that properly prepared PMMA (through oxidation of monomer) exhibited a substantial increase in refractive index after irradiation with UV light at 325nm (He-Cd^+ Laser) or 365nm (Hg arc). A subsequent report related to the photosensitivity of PMMA is a paper on dye-doped polymer laser [7].

In the recent research carried out at the University of New South Wales, photosensitivities of various PMMA-based Polymer Optical Fibres (POF) were investigated [8,9]. These include PMMA POFs made from undoped, dye-doped or oxidated preforms under various irradiation wavelength, intenisty and time. However, the understanding and knowledge to the mechanism of photosensitivity and the Bragg grating formation in polymer optical fibres so far have been very limited.

In this paper, we report several interesting observations and relevant experimental results from our systematic investigation on the growth dynamics of polymer fibre Bragg gratings. For the first time, we report the observation of a threshold in UV exposure or fluence in the grating creation process. The threshold distinguishes two types of fibre gratings that have quite differently properties and performance. With the better knowledge of a grating creation process from this investigation, we have recently produced PMMA-based polymer fibre Bragg gratings with the best results ever achieved: a reflectivity better than 0.998 and a linewidth less than 0.5nm [10].

2. Basic relations of optical fibre gratings

Here we introduce some basic relations that will be used to work out the refractive index change, or photosensitivity, in polymer fibre introduced in the grating fabrication process. The schematic diagram of a fibre Bragg grating is shown in Fig.1. Here an incident light launched into the fibre section written with a Bragg grating in the core is highly reflected within a narrow band around a Bragg wavelength. The Bragg wavelength is determined by the constructive interference, i.e. the in-phase condition, of partial reflections from each part of the grating.

Within a simple model of periodic index change, the in-phase condition can be directly linked to the condition giving the Bragg reflection of a grating. The is the famous Bragg condition widely used and it can be obtained from the usual energy and momentum conservation laws involving light and matter interaction.

The momentum conservation related to the grating reflection can be explicitly expressed as

$$\mathbf{K} + \mathbf{k_i} = \mathbf{k_r} \qquad (1)$$

where **K, $\mathbf{k_i}$** and **$\mathbf{k_r}$** are the wave-vectors of the grating, the incident light and the reflected light respectively. This relation is depicted in Figure 2. The vector **K** has a magnitude given by

$$K = \frac{2\pi}{\Lambda} \tag{2}$$

where Λ is the grating period. For optical fibre gratings, the magnitudes of **$\mathbf{k_i}$** and **$\mathbf{k_r}$** , are usually referred to as propagation constants, and are respectively given by

$$\beta_i = \frac{2\pi}{\lambda_i} \mathrm{n_{eff}} \quad \text{and} \quad \beta_r = \frac{2\pi}{\lambda_r} \mathrm{n_{eff}} \tag{3}$$

where n_{eff} is the effective refractive index of the optical fibre mode (usually the fundamental mode). The incident and reflected waves are both along the fibre axis and in opposite directions to each other. To satisfy the momentum conservation condition, the direction of **K** is also along the fibre axis and in the direction of the reflected wave-vector. Under the energy conservation law, the incident wave and reflected wave should have the same energy, i.e.

$$\hbar\omega_\mathrm{i} = \hbar\omega_\mathrm{r} \tag{4}$$

for the same wavelength and we assume there is no energy transfer from one wavelength to another and no radiation loss; $\hbar=2\pi h$ where *h* is the Planck's constant. Hence we can write for frequency

$$f_i = f_r = \mathrm{f}_B \tag{5}$$

and for wavelength

$$\lambda_\mathrm{i} = \lambda_\mathrm{r} = \lambda_\mathrm{B} \tag{6}$$

with

$$\mathrm{f_B}\lambda_\mathrm{B} = \mathrm{c} \tag{7}$$

where c is the light velocity and λ_B denotes the Bragg wavelength. Thus from both the energy and momentum conservation conditions, we can arrive at the Bragg condition

$$\mathrm{N}\lambda_\mathrm{B} = 2\mathrm{n_{eff}}\Lambda \tag{8}$$

where N is an integer representing the order of the interaction. In most practical cases of our interest, N=1. The Bragg condition provides the simple and yet very important relation between the Bragg wavelength and the grating parameter --the period Λ of the index variation.

The reflection and transmission in a Bragg grating of an optical fibre are described by the Coupled Mode Theory (see for example [11]). Following the simple analysis of [12], we consider a single fibre with a Bragg grating of length L. We eliminate the common propagation constant (say β_0) and

only consider the difference δ between β_0 and the actual propagation constant. We let A and B represent the complex amplitudes of the forward and backward propagating modes and then set

$$A(z)=R(z)\exp(j\delta z) \tag{9}$$

and

$$B(z)=S(z)\exp(-j\delta z). \tag{10}$$

This leads to

$$R'[z] + j\,\delta\,R[z] = -j\,\kappa\,S[z] \tag{11}$$

and

$$S'[z] - j\,\delta\,S[z] = j\,\kappa\,R[z]. \tag{12}$$

Reorganising the coupled equations, we have

$$R''[z] + (\delta^2-\kappa^2)R[z] =0 \tag{13}$$

and

$$S''[z] + (\delta^2-\kappa^2)S[z] =0 \tag{14}$$

Using these equations, it is easy to prove that

$$|R(z)|^2 - |S(z)|^2 = \text{constant} \tag{15}$$

The modulation Δn in the refractive index determines the Bragg (forward- to- backward) coupling coefficient. For sinusoidal index change along the fibre axis, the coupling coefficient is given by

$$\kappa = \frac{\pi\Delta n}{\lambda} \tag{16}$$

with λ the signal light wavelength. The frequency offset is $\delta = k - k_B$, where $k = 2\pi/\lambda$ is the signal wave-number in free space and $k_B = 2\pi/\lambda_B$ is the centre Bragg wave-number and λ_B is the Bragg wavelength.

The range of frequencies where the light is reflected, i.e. the band-gap, has a width proportional to κ. Within the band-gap, i.e. for frequency offsets δ satisfying $\delta^2 < \kappa^2$, almost all the light is reflected, but outside this range, i.e. $\delta^2 > \kappa^2$, the fraction reflected is small.

Physically, this means that each element of power decrease in the forward propagating mode is added to the reflected mode, thus ensuring that the difference remains constant. We have the boundary conditions R(0)=1 and S(L)=0. It can be shown that arg[S(z)] is also a constant. The result

is that, inside the band-gap, both |R| and |S| decrease monotonically as z increases and the curves are similar, as almost all the light is reflected.

However, outside the band-gap, $|R|^2$ and $|S|^2$ are oscillating functions of z, since standing waves are set up in the grating. In this range, |R| remains high for all values of z, while |S| is always fairly small. This means that the constant value of ($|R(z)|^2$ - $|S(z)|^2$) is now larger than it was when the parameters were within the band-gap.

Within the band-gap: Within the band-gap ($\delta^2 < \kappa^2$), we let $q^2 = \kappa^2 - \delta^2 > 0$. The exact solution of R(z) to the above system can be easily found. We write R(z) in the form

$$R = R_r + j\, R_i \tag{17}$$

The exact solution can be expressed as R_r and R_i

$$R_r = H \{ \kappa^2 \cosh[q\,(z-2L)] + (q^2 - \delta^2) \cosh[q\, z] \} \tag{18}$$

$$R_i = -2\, q\, \delta\, H \sinh[q\, z] \tag{19}$$

where the constant H is

$$H = \frac{1}{2\left(q^2 \cosh^2(qL) + \delta^2 \sinh^2(qL)\right)} \tag{20}$$

The exact solution of S(z) to the above system within the band-gap ($\delta^2 < \kappa^2$) can also be found, in the form

$$S = S_r + j\, S_i \tag{21}$$

with

$$S_r = -2\, \kappa\, q\, H \cosh[qL] \sinh[q\,(z-L)] \tag{22}$$

$$S_i = -2\, \kappa\, \delta\, H \sinh[qL] \sinh[q\,(z-L)] \tag{23}$$

The reflectivity from a fibre Bragg grating can be worked out

$$\text{Reflectivity} = \left|\frac{S(0)}{R(0)}\right|^2 = \frac{\kappa^2 \sinh^2(qL)}{\delta^2 \sinh^2(qL) + q^2 \cosh^2(qL)} \tag{24}$$

As a simple example, we consider the case when the frequency offset is $\delta=0$, i.e. the incident wavelength is at the centre of the band-gap. A simple expression for reflectivity is obtained

$$\text{Reflectivity} = \tanh^2[\kappa L]. \quad (25)$$

It is obvious that the reflectivity is increased with the increase of both the refractive index change Δn (since $\kappa=\pi\Delta n/\lambda$) and grating length L.

Outside the band-gap: The exact solution of R(z) to the above system, when outside the band-gap ($p^2 = \kappa^2 - \delta^2 > 0$), can be obtained in similar manner to Equation (17)

$$R=R_r+ j\, R_i$$

where

$$R_r = \cos[p\, z] - G\, p \sin [p\, z] \cos[p\, L] \quad (26)$$

$$R_i = G\, \delta \sin [p\, z] \sin[p\, L] - (\delta/p) \sin [p\, z], \quad (27)$$

where $p^2 = \delta^2 - \kappa^2 > 0$, and the constant G is

$$G = \frac{\kappa^2 \sin(pL)}{p\left(p^2 \cos^2(pL) + \delta^2 \sin^2(pL)\right)} \quad (28)$$

We may define the effective change in the local propagation constant caused by the grating to be

$$\beta(z) = \frac{d}{dz}\arg[R(z)] = \frac{d}{dz}\arctan\left[\frac{R_i}{R_r}\right] \quad (29)$$

The propagation constant is related to the dispersion of the grating. This is very important for fibre grating in a number of applications such as dispersion compensation in optical fibre transmission lines. Here it is an oscillating function which has one or more cycles over the grating length, depending on the parameters. Its minimum value is $-\delta$, so the effective change in propagation constant of the initial complex mode [A(z)] , viz. $\beta(z) + \delta$, has a minimum of 0. Its maximum is of order κ. Thus the propagation constant is periodic and the magnitude of its modulation is of the order of the grating coupling coefficient.

3. Polymer fibre Bragg grating fabrication

We made single-mode POFs based on the preform techniques that was used described in [13]. The POF samples used in the experiments has an outer diameter of 133 μm and a core diameter of 6 μm. The difference in the refractive index between the core and the cladding is measured to be 0.0086, by employing a transverse field fringe method using an interferometric microscope.

The fibre Bragg grating was fabricated using the setup shown in Fig.2. This setup uses the techniques of both phase mask and Sagnac interferometer. A π phase mask is placed close to the fibre sample and the a UV laser beam of suitable wavelength is needed to induce a certain photosensitive process in the polymer.

The period of the phase mask is 1.06μm, which was designed for direct grating writing using 248 μm wavelength. The UV writing beam was from a frequency-doubled MOPO pumped by a frequency-tripled Nd:YAG laser. The UV laser beam was not focused and has an effective spot size of 3mm, pulse energy of 3 mJ with a pulse width of 5ns at 10Hz repetition rate. The wavelength for gratings fabrication in our case is not the designed wavelength of the phase mask at 248nm. Hence the zeroth diffraction order from the phase mask is pretty high and this zeroth is detrimental to the formation of Bragg gratings [14]. Therefore we use three prisms to construct a modified Sagnac interferometer where the two first-order diffraction beams form the required interference pattern for the gratings, while the zeroth order is blocked. This configuration is an adaptation of the transverse method developed by Meltz, Morey and Glenn [15] with the introduction of a static ring interferometer based on the patent invented by Ouellettee [16]. In the course of gratings inscription, we use an Advantest Q8384 optical spectrum analyzer and an ANDO AQ63128 optical spectrum analyzer to monitor its transmission and reflection spectra at the same time. We employ a broadband light source for the online monitoring and characterisation of grating fabrication process.

4. Growth dynamics of POF gratings

Using the experimental setup described above, we investigated the growth dynamics of polymer fibre grating. The transmission and reflection spectra of POF gratings at different UV exposure time are shown in Fig.3(a) and (b). We observed remarkable change in both reflection and transmission at wavelength around 1574nm as the POF under UV exposure. From Fig.3(a) it is obvious that the rejection level at the band-gap (Bragg wavelength) in the transmission spectrum increases slowly until 62 minutes of exposure. As the exposure time continues from 62 minutes to 85 minutes, the rejection level increases significantly and drastically. With 67 minute exposure, the rejection level is about double of that with 62 minute exposure. At the exposure time of 85 minutes, the transmission at the Bragg wavelength even goes down low to the noise level. In the last 23 minutes, the rejection level is increased from approximately 4dB at the 62 minute to about 30dB at the 85 minute.

From the reflection spectra in Fig.3(b), it is obvious that there are significant side lobes. Moreover, as the reflection level at Bragg wavelength increases, the amplitude of side lobes also increases. The side lobes are due to the resonance of multiple reflections to and from opposite ends of the grating regions. In order to suppress the side lobes, an apodized refractive index profile have to be introduced. However, it is not our main concern in this work and no experiment has been done to confirm this yet.

The transmission and reflection spectra of the POF gratings after 85 minute exposure are also recorded and displayed in Fig.4. It is clear from the transmission spectra in Fig.4(a) that the transmission is rapidly deteriorated with excessive exposure – both the loss at short wavelengths and the grating bandwidth have increased remarkably. At the same time, from the reflection spectra in Fig.4(b) that the reflection or rejection level decreased from the maximum that is achieved with about 85 minute exposure.

Using the basic relations Eq.(16) and Eq.(25) that were described in Section 2, the grating reflectivity and the refractive index modulation Δn induced by UV at different exposure time were estimated from the experimental transmission spectra. The corresponding data are summarised in Fig.5. From the Δn vs exposure time curve, it is apparent that a distinctive threshold exists at the time around 62 minute. Below the threshold exposure time, Δn increases almost linearly. Whereas above the threshold exposure time, Δn increases drastically until reaching a maximum value. In the case of our experiment, the value of Δn at 85 minute became about 5 times as greater as that at 62 minute. In this case, an index modulation as high as 10^{-3} was achieved. With excessive exposure after 85 minute, Δn decreased gradually.

From the experimental results above, we conclude that there also exists an optimal UV exposure level for the POF fibre to achieve the maximum index modulation. With excessive level of exposure, the index modulation will reduce and the rejection bandwidth will increase.

By optimizing the exposure conditions we were able to achieve POF gratings with large rejection value and narrow bandwidth. The transmission spectrum of a POF grating fabricated with 85 minute' exposure is shown in Fig.6. The spectrum indicates at least 28dB (limited by the resolution of the measurement system) rejection was achieved at the Bragg wavelength, corresponding to less than 0.2% of the light is transmitted. In this case, the bandwidth of less than 0.5nm is achieved.

We also found that the Bragg wavelength of POF grating shifts to the blue part of the spectrum in the process of grating fabrication. If the type I gratings is formed mainly due to the refractive index change in the core, the wavelength λ_B will be determined by

$$\lambda_B = (1+\Delta n / n)\lambda_{Bo} \tag{30}$$

where n is the effective refractive index of the core and λ_{Bo} is the nominal Bragg wavelength when the index modulation is not considered. From Eq.(30), λ_B increases with the index modulation Δn. If λ_B shifts toward short wavelengths, the index modulation Δn is negative, i.e. the refractive index change induced by the POF gratings is negative. In Fig.7, the Bragg wavelength of a POF grating versus the UV exposure time is shown. The Bragg wavelength of the gratings decreased about 0.5nm in one and a half hour. Hence Δn must be negative. This negative change of index is also shown in Fig.5.

Comparing our experimental results on growth dynamics of POF gratings with that of Ge doped silica fibre gratings previously reported, it is interesting to reveal that their Δn versus UV exposure behavior is very much similar.

In the process of silica fibre grating fabrication, it is well known that there is a threshold of exposure, below which the index modulation grows linearly. When above the threshold point, the induced index modulation increases dramatically and becomes saturated [17]. Because of these similarity, in the following context, we follow the nomenclature used Ge-doped silica fibre gratings to categorize the POF gratings. Hence we refer the POF gratings, as depicted in Fig.5 that are fabricated below and above the threshold (i.e. low and high index modulation), as type I and type II grating, respectively.

We had a detailed review on the transmission and reflection spectra for type I POF gratings from our experiment data. We found that the reflection spectra, while below the exposure threshold as described above, are in complimentary to the transmission ones. This means that there are no significant excess losses due to absorption or coupling into the claddings. This is strikingly similar to the fundamental characteristics of type I silica fibre gratings, which are characterized by the UV-induced refractive index change in the core resulted from the material photosensitivity. Hence, in terms of transmission and reflection characteristics, the type I POF grating resembles the type I silica grating.

Furthermore, we carried out morphology test of the type II POF gratings using optical microscope. The morphology photo is displayed in Fig.8. From the morphology photo, we could see clearly that there is a damaged track at the core-cladding interface. The damage can also explain the strongly coupling of the short wavelength into claddings. The damage might be caused by the interaction of UV pulse with electrons in the conduction band, resulting in rapid heating to above the melting point. This observation strongly suggesting that the damage may be responsible for the large index modulation of the type II POF gratings. Again, this is similar to the damage that has been revealed in the type II silica fibre gratings [17]. Our experimental observation here provides a clear evidence that, regardless of their respective formation process and mechanism, the type II POF grating and silica grating have similar characteristics and that their characteristics are both possibly linked to damage grating formation.

5. Conclusions

We carried out a detailed investigation on the growth dynamics of POF Bragg gratings. We observed for the first time that the dynamic growth, formation and resulting characteristics of POF Bragg grating are remarkably similar to that of silica fibre Bragg gratings. Of course this similarity could be merely superficial since the underlying mechanism or process could be vastly different because of totally different material systems. In particular, we observed that there is a distinctive threshold in UV exposure. The threshold distinguishes two different grating formation stages. In the

first stage when the exposure is under the threshold, the index modulation grows slowly and linearly, and the transmission and reflection spectra is complimentary to each other without significant excess loss. Whereas in the second stage when exposure is above the threshold, the index modulation increases rapidly and dramatically, until reaching a saturation value, large losses at short wavelengths occur, bandwidth increase and distinctive damage in the core and cladding interface induced.

Acknowledgments: This work is partly supported by Australian Research Council. The authors would like to thank T Whitbread and G. H. Gamage for their assistance in laser operation.

6. References

[1]. K. O. Hill, Y. Fuji, D. C. Johnson, and Kawasaki B. S. "Photosensitivity in optical fibre waveguides: Application to reflection filter fabrication," Appl. Phy. Lett., vol. 32, pp647-649, 1978

[2]. L. Dong, P. Hua, T. A. Reekie, and P. St. J. Russell, "Novel add/drop filters for wavelength division multiplexing optical fibre system using a Bragg grating assisted mismatched coupler," IEEE Photonics Technol. Lett., vol. 8, pp1656-1658, 1996

[3]. C. R. Giles, T. Strasser, K. Dryer, and C. Doerr, "Concatenated fibre grating optical monitor," IEEE Photonics Lett., vol. 10, pp1452-1454, 1998

[4]. S. Savin, "Tunable mechanically induced long-period fibre gratings," Opt. Lett., vol 25, pp710-702, 2000

[5]. G. D. Peng, "Prospects of polymer optical fibres and gratings in sensing", invited paper, Proc. of the 15th International Conference on Optical Fibre Sensors, Portland, USA, pp71-74, 2002

[6]. W. J. Tomlinson, I. P. Kaminow, E. A. Chanderross, R. L. Fork and W. T. Silfvast, "Photoinduced refractive index increase in poly(methyl methacrylate) and its applications", Appl. Phys. Lett., vol.16, no.12, 486-488, 1970

[7]. I. P. Kaminov, H. P. Weber, E. A. Chanderross, Appl. Phys. Lett. vol.18, 497, 1971

[8]. G. D. Peng, Z. Xiong, and P. L. Chu, "Photosensitivity and grating in dye-doped polymer optical fibres," Optical Fibre Technology, vol. 5, pp242-251, 1999

[9]. Z. Xiong, G. D. Peng, B. Wu, and P. L. Chu, "Highly tunable Bragg gratings in single mode polymer optical fibres," IEEE Photonics Techno. Lett., vol. 11, pp352-354, 1999

[10]. H. Y. Liu, G. D. Peng and P. L. Chu, "Polymer Fiber Bragg Gratings with 28dB Transmission Rejection", to appear in IEEE Photonics Technology Letters, July 2002

[11]. A. Yariv, "Optical Electronics in Modern Communications", Oxford University Press, New York, Chapter 13, 1997

[12]. A. Ankiewicz, Z. Wang and G. D. Peng, "Analysis of narrow bandpass filter using coupler with Bragg grating in transmission", Optics Communications, vol.156, pp.27-31, November 1998

[13]. G.D. Peng, P.L. Chu, X. Lou and R.A. Chaplin, "Fabrication and Characterisation of Polymer Optical Fibres," J. Electronics & Electrical Engineers Australia, pp.289-296, September 1995

[14]. Z. Xiong, G. D. Peng, B. Wu and P. L Chu, "Effects of the zeroth-order diffraction of a phase mask on Bragg gratings," J. Lightwave Technol., vol 17, pp. 2361-2365, 1999

[15]. G. Meltz, W. W. Morey, W. H. Glenn: "Formation of Bragg gratings in optical fibres by a transverse holographic method," Opt. Lett., Vol.14, pp.823-825, 1989

[16]. F. Ouellette, University of Sydney Patent Cooperation Treaty AL/96/00782

[17]. J. L. Archambault. L. Reekie and P. St. J. Russell, Electron. Lett., 29, 453, (1993)

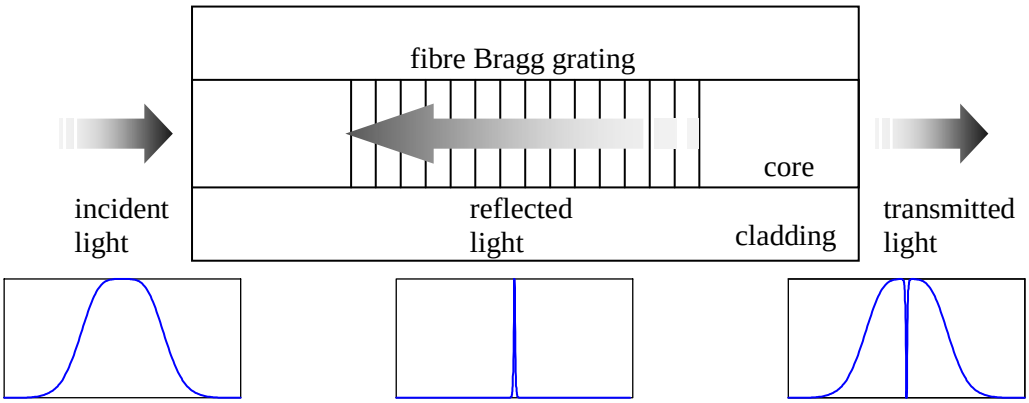

Fig.1 Schematic diagram of a fibre Bragg grating.

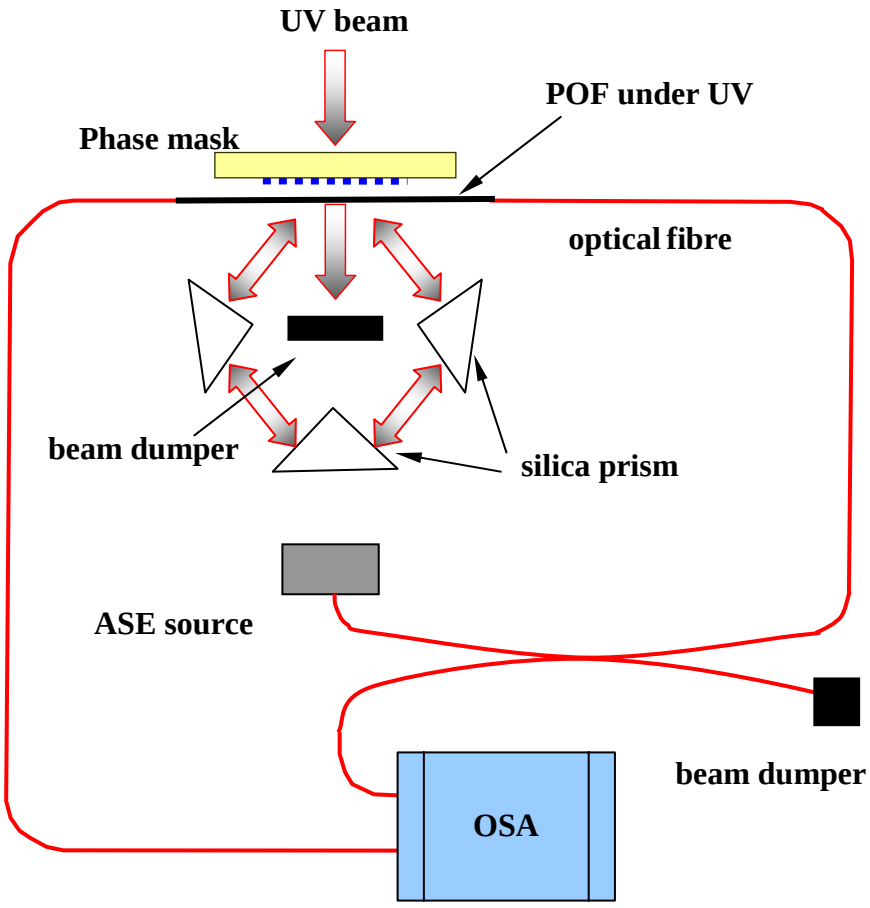

Fig.2 Setup for POF Bragg gratings fabrication.

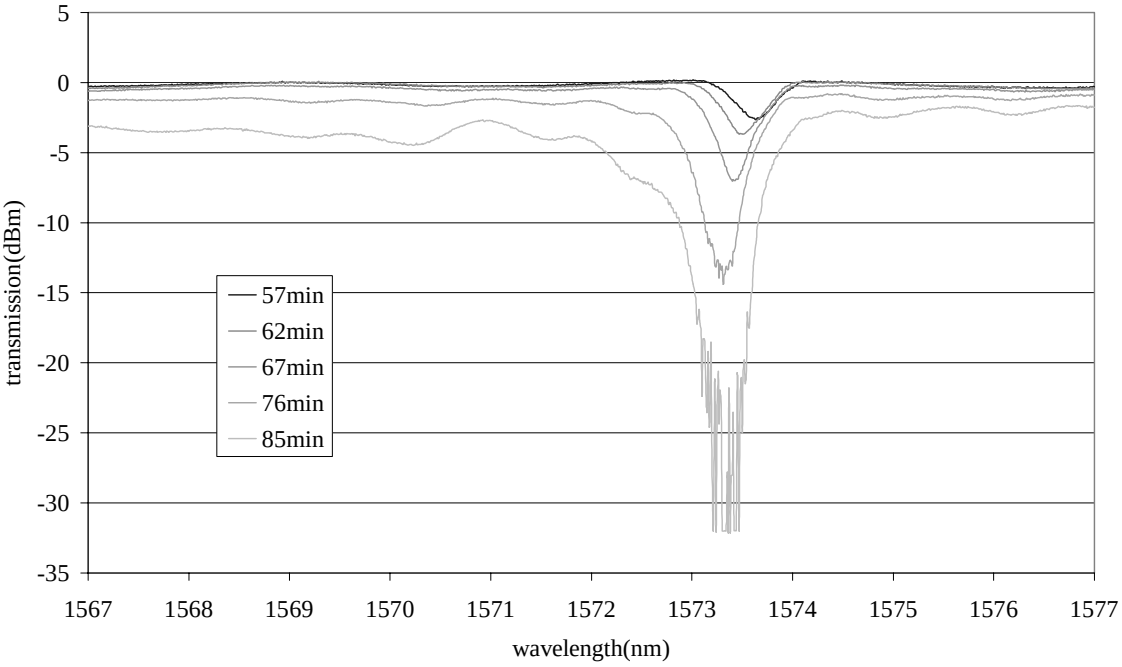

(a)

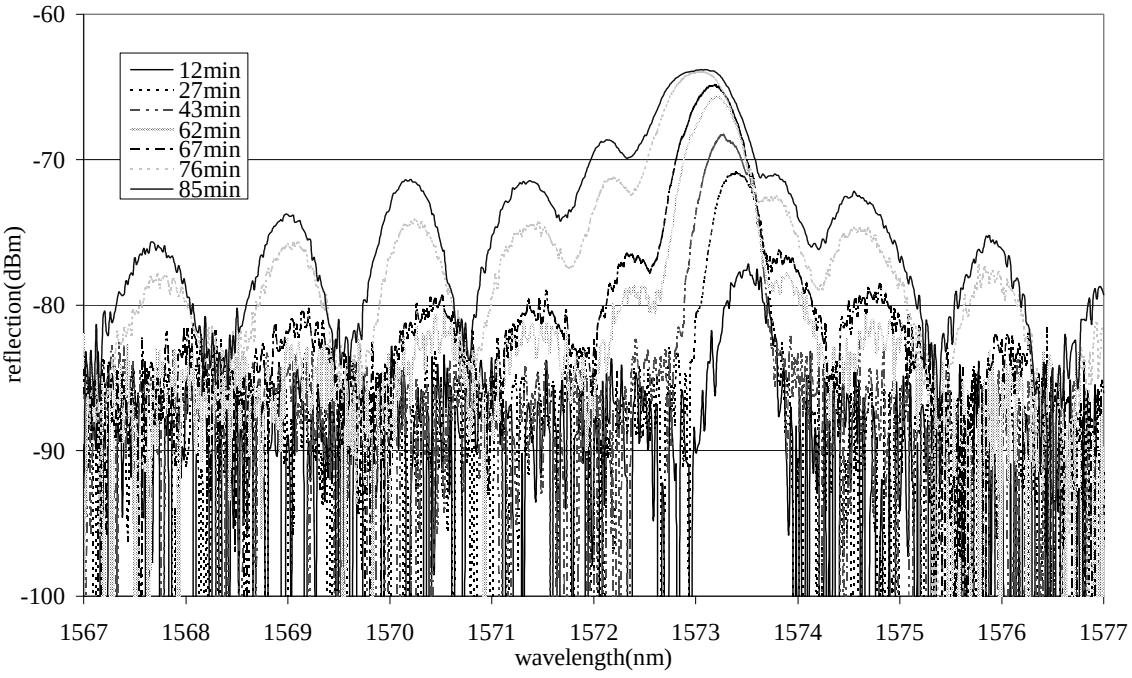

(b)

Fig.3 The transmission (a) and reflection (b) spectra of POF gratings at different UV exposure time

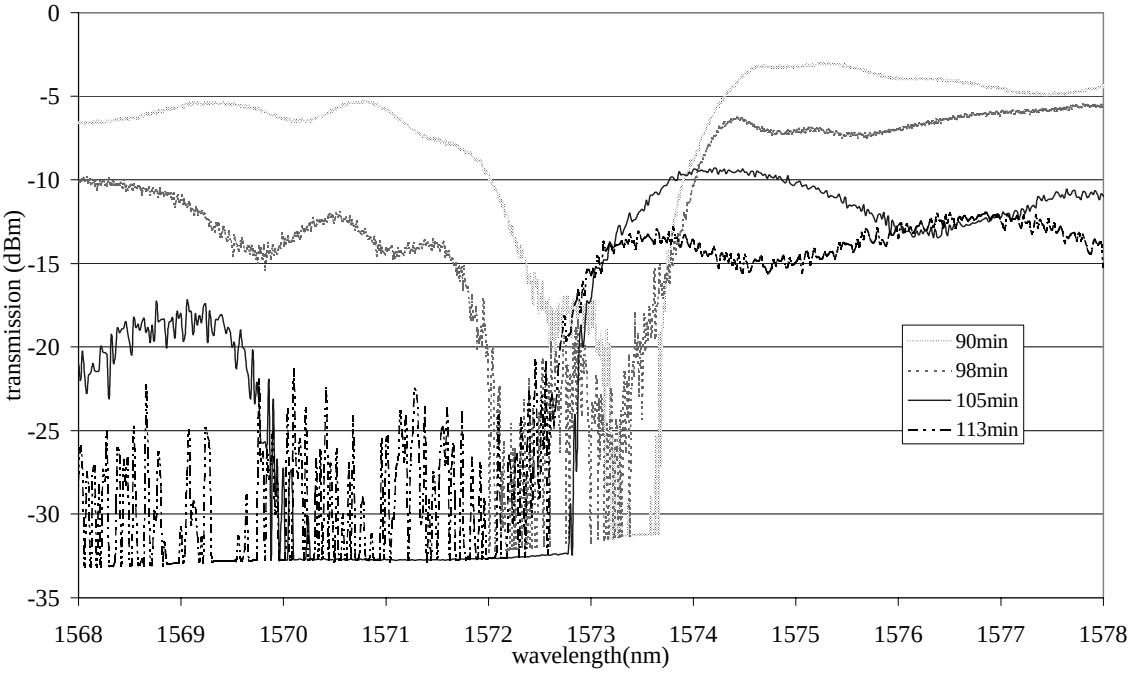

(a)

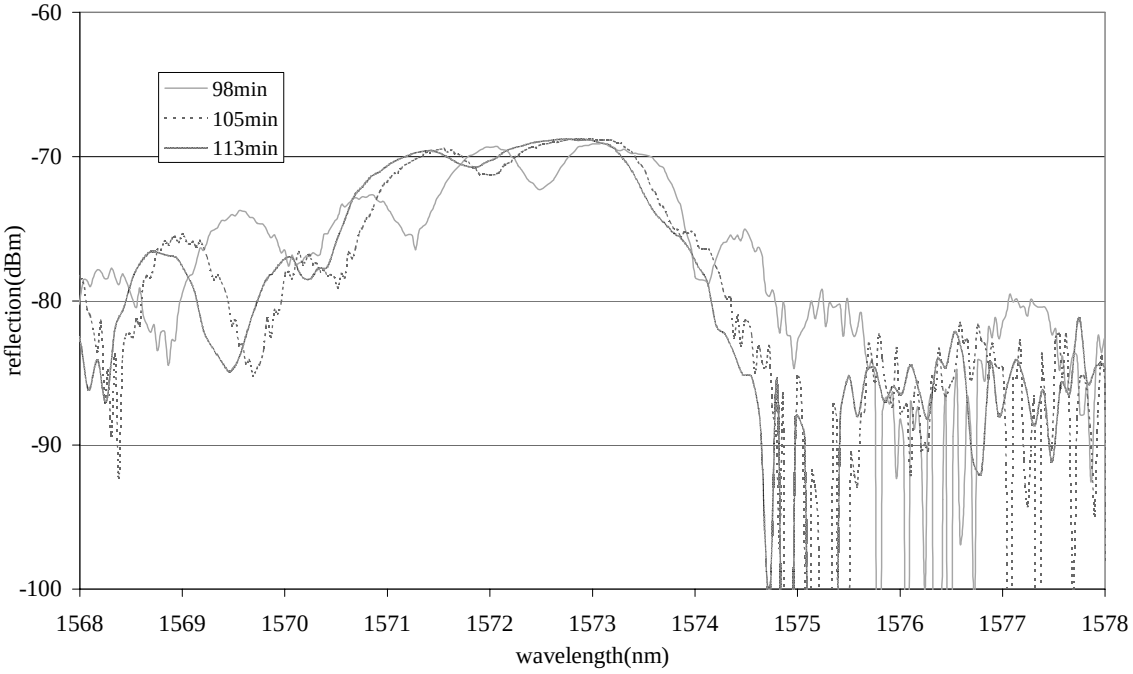

(b)

Fig.4 Transmission (a) and reflection (b) spectra of POF gratings when over-exposed after 85 minutes.

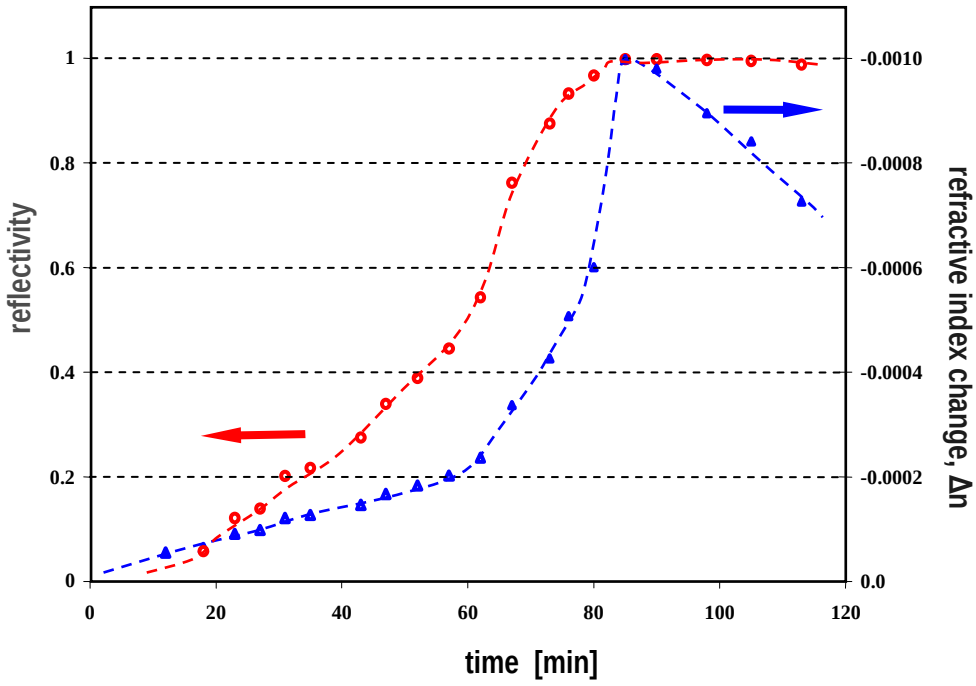

Fig.5 Reflectivity and refractive index modulation of POF Bragg gratings at different exposure time

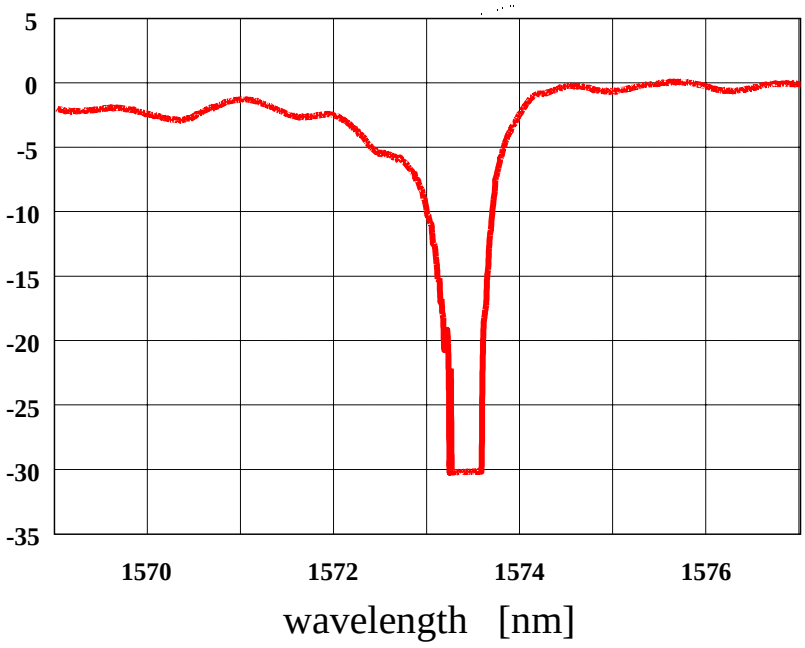

Fig.6 Transmission spectrum of POF Bragg gratings at optimized UV exposure time with 28dB transmission rejection and a line width of less than 0.5nm

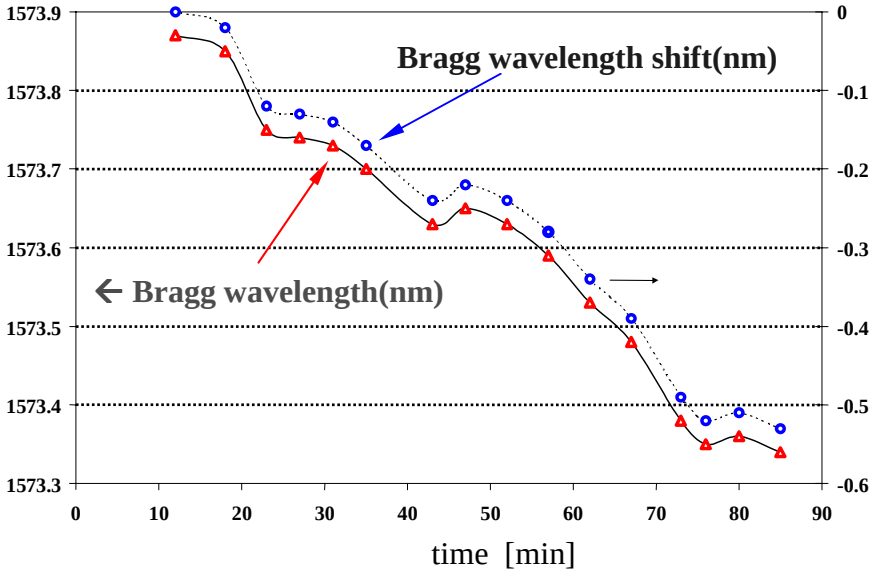

Fig. 7 POF Bragg wavelength shift in the course of inscription.

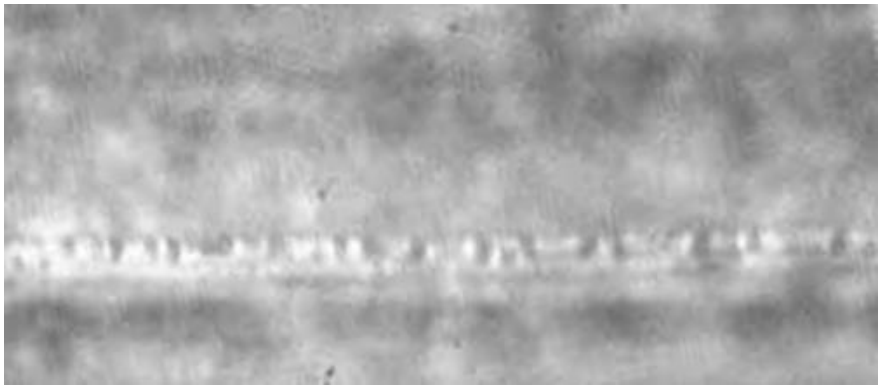

Fig.8 Optical morphology of a type II POF grating.